Progress In Electromagnetics Research M, Vol. 21, 19–32, 2011

A PRINTED LOG-PERIODIC TREE-DIPOLE ANTENNA (PLPTDA)

S. Lin [1, 2, *], S. Luan [2], Y. D. Wang [2], X. Luo [2], X. Han [2], X. Q. Zhang [2], Y. Tian [2], and X. Y. Zhang [2]

[1]Electronic Science and Technology Post-doctoral Research Center, Harbin Institute of Technology, Harbin 150080, China

[2]School of Electronics and Information Engineering, Harbin Institute of Technology, Harbin 150080, China

Abstract—A miniaturized printed log-periodic fractal dipole antenna is proposed. Tree fractal structure is introduced in an antenna design and evolves the traditional Euclidean log-periodic dipole array into the log-periodic second-iteration tree-dipole array (LPT^{2}DA) for the first time. Main parameters and characteristics of the proposed antenna are discussed. A fabricated proof-of-concept prototype of the proposed antenna is etched on a FR4 substrate with a relative permittivity of 4.4 and volume of 490 mm × 245 mm × 1.5 mm. The impedance bandwidth (measured VSWR < 2) of the fabricated antenna with approximate 40% reduction of traditional log-periodic dipole antenna is from 0.37 to 3.55 GHz with a ratio of about 9.59 : 1. Both numerical and experimental results show that the proposed antenna has stable directional radiation patterns and apparently miniaturized effect, which are suitable for various ultra-wideband applications.

1. INTRODUCTION

As ultra-wideband technology is widely applied to communication system, ultra-wideband antennas, with ultra-wideband, small volume and high gain, are highly desired. Therefore, in order to meet the requirements, many researchers provide a large number of solutions. These solutions mainly include: a) ultra-wideband omni-directional antenna, of which wafer monopole antenna [1, 2] is the representative, and various special-shaped-pole antennas [3–5], which are mainly used

Received 1 August 2011, Accepted 6 September 2011, Scheduled 14 September 2011

* Corresponding author: Shu Lin (linshu@hit.edu.cn).

in the frequency band from 3.1 to 10.6 GHz (approved by FCC), but generally, this kind of antenna is omni-directional antenna with low gain, which could be arranged as an array to improve the gain, however, the feed network of the array is too difficult to solve; b) wide slot antennas [6, 7], including all kinds of wide-slot coupled feed antennas whose gains are low; c) antennas with resistance gradual changing structure, including some ultra-wideband directional antennas, such as Vivaldi antenna [8], TEM horn antenna [9], ridged horn antenna [10], etc. However, most of these kinds of antennas are limited by their large volume for certain applications; d) frequency independent antennas, including equiangular and Archimedean spirals, log-periodic dipole antennas, and so on. This kind antenna could cover ultra-wideband with a ratio of above 5 : 1 with high gain. However, the volume is large as well.

Microstrip antennas have some attractive advantages such as small volume, very low-profile, light weight, easy fabrication and constant directional radiation patterns, which have been widely used in designing miniaturized antennas. Since the development of printed circuit technology, many traditional antennas could be made into corresponding printed antennas, such as printed monopole antennas [11], printed log-periodic dipole antennas [12], etc. Fractal theory is a quite active mathematic branch of nonlinear science, and the research objects of which are certain unsmooth or non-differentiable geometries in nonlinear systems and nature. Fractal technology has been extensively applied to every aspect of science and engineering field, and one significant branch of which is fractal electrodynamics. Meanwhile, fractal antenna is one of fractal electrodynamics' applications. Fractal structure has self-similarity and space filling characteristics which could realize the miniaturized antenna design. In antenna's design, the usual fractal structure is Koch fractal [13], Tree fractal [14], Hilbert fractal [15], etc.

In order to achieve the miniaturized log-periodic dipole antenna (LPDA), this paper introduces the 2nd-iteration tree fractal dipoles as the basic structural elements of an ultra-wideband log-periodic 2nd-iteration tree-dipole array (LPT^2DA) for the first time. The configuration of the proposed LPT^2DA is described in Section 2. The numerical and measured results are presented and discussed in details in Section 3, observing the correctness of the design idea. This paper is concluded in Section 4. The reduction of conductor's length in polarization direction is the most significant achievement in this paper.

2. LPT^{2}DA ANTENNA DESIGN

2.1. Tree Fractal Dipole

Tree fractal structure is created in iteration method. The procedure is as followings: firstly, divide a straight wire (noted in iteration as "T0") of length l into three segments, then put two segments of length $l/3$ intersecting at a angle 90° on two sides of the wire at two trisection points respectively, forming a combination whose total length is $5l/3$. After the first iteration, the 1st-iteration tree fractal curve is obtained, called "T1". By repeating this procedure, for each segment more times of iteration (T2, T3, and so on) can be obtained. Fig. 1 shows the procedure of this tree fractal structure. After each iteration, the total length of the temp structure is 5/3 times of the previous one. The advantage of this fractal structure is that the fractal extends to both sides of the main wire. The space filling characteristic of tree fractal is better than that of the fractal structure which extends only to one side of the main wire (such as Koch fractal).

The fractal dimension aspect can also explain the space filling performance. The introduction of fractal dimension breaks through the limitation that the dimension is an integer. The Hausdorff dimension usually used currently is adopted to calculate the fractal dimension of the treelike fractal graphic. The definition of the Hausdorff dimension is: for some object, the new object K times of the old object can be obtained if it is amplified L times along some independent direction. Then the dimension of the object is $D_H = \ln K / \ln L$. Thus, the dimension of the treelike fractal graphic $D_H = \ln 5 / \ln 3 = 1.46$. The fractal dimension of the Koch graphic is only $D_H = \ln 4 / \ln 3 = 1.26$.

Tree fractal dipole is evolved from tree fractal structure, and the configuration of which is shown in Fig. 2. The simulated result shows that, when the oscillator arm lengths of T0, T1 and T2 are all 67.5 mm, the resonant frequencies of them is respectively 1 GHz,

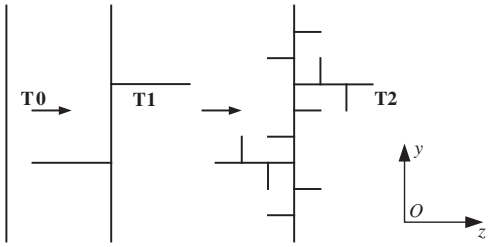

Figure 1. Procedure of tree fractal structure.

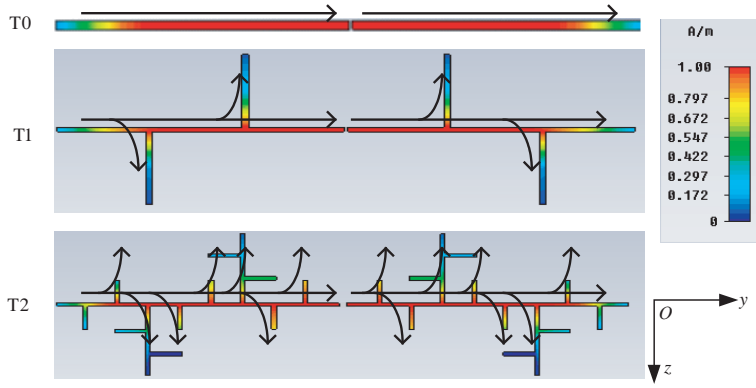

Figure 2. Configuration of tree fractal dipole and surface current.

0.87 GHz and 0.78 GHz. It means that, with the same conductor's length in co-polarization direction, the higher the degree of iteration is, the lower the first resonant frequency is. But the rate of the first resonant frequency's decline becomes slower as the iteration times increase. From this, we could speculate that at last the first resonant frequency would be a constant value (in Fig. 2, the arrows show the main radiation direction of surface current). The decline of the first resonant frequency indicates that, with the same operating frequency, the size of tree fractal dipole would be smaller than that of traditional dipole. But when the iteration times increase to some extent, the fine size, formed by tree fractal structure, would be similar to cross-sectional area of metal. Then the antenna surface current does not accord with the surface current distribution condition of traditional tenuous dipole antenna, and the fractal miniaturized method does not work.

From the current flow (shown in Fig. 2), it can be seen that the current on the fractal dipole will generate the radiation field with cross polarization in z direction. However, the antenna's radiation field of main polarization is in y direction, thus the polarization direction of the treelike fractal dipole is in the same direction. And it determines the polarization direction of the log-periodic antenna composed of the treelike fractal dipole is also in y direction.

2.2. Printed Log-periodic Tree-fractal Dipole Antenna

The printed log-periodic tree-fractal dipole antenna (PLPTDA) is composed of an array of log-periodic tree-fractal dipoles and a microstrip feeding line. The proposed antenna is designed by a semi-

empirical way like the design procedure of traditional LPDA. Firstly, the LPDA basic parameters are determined by operating frequency and gain. Secondly, the dipoles of LPDA are processed by tree-fractal method. Lastly, optimize the parameters, such as spacing factor.

2.2.1. Traditional Printed Log-periodic Dipole Antenna

Design of Euclidean LPDA has been very mature, and the key of which is the selection of some special parameters, including scaling factor τ, spacing factor σ and the number of dipoles N, that is,

$$\tau = L_{n+1}/L_n = d_{n+1}/d_n \tag{1}$$

$$\sigma = d_n/(4L_n) \tag{2}$$

$$N = 1 - \ln B_s / \ln \tau \tag{3}$$

In (1) L_n is the length of the n^{th} pole, d_n is the distance between the nth pole and the $(n+1)^{\text{th}}$ pole, $B_s = B_0 B_a$, B_0 is the operating frequency, $B_a = 1.1 + 30.7\sigma(1-\tau)$.

According to the relation between gain value and τ, σ, chose appropriate τ and σ. The number of dipoles is determined by operating frequency. τ is from 0.8 to 0.95, and σ is from 0.08 to 0.15. The parameters of traditional LPDA are $\tau = 0.85$, $\sigma = 0.12$, $l_1 = 2L_1 = \lambda_{\max}/2 = 375\,\text{mm}$, $N = 16$, $l_i/a_i = 125$, $i = 1, 2, 3\ldots$, and the start frequency is 0.4 GHz. The structure of Euclidean LPDA is shown in Fig. 3(a).

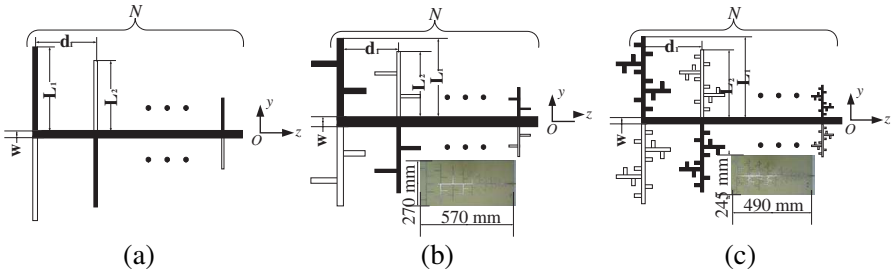

Figure 3. Configuration of LPDA, LPT[1]DA and LPT[2]DA (■ Top of substrate, □ Bottom of substrate). (a) LPDA, $N = 16$, $L_1 = 187.5\,\text{mm}$, $d_1 = 90\,\text{mm}$, $w = 3\,\text{mm}$, $\sigma = 0.12$, $\tau = 0.85$. The antenna size is $555\,\text{mm} \times 400\,\text{mm}$. (b) LPT[1]DA, $N = 16$, $L_1 = 133\,\text{mm}$, $d_1 = 79.8\,\text{mm}$, $w = 3\,\text{mm}$, $\sigma = 0.15$, $\tau = 0.85$. (c) LPT[2]DA, $N = 16$, $L_1 = 120\,\text{mm}$, $d_1 = 76.8\,\text{mm}$, $w = 3\,\text{mm}$, $\sigma = 0.16$, $\tau = 0.85$.

2.2.2. Design of Printed Log-periodic 1-iteration Tree-fractal Array (PLPTDA)

Based on the designed Euclidean LPDA, 1st-iteration tree-fractal (noted as T1) dipoles are used to take the place of dipoles. The length of fractal dipoles in co-polarization direction is shorter than that of traditional dipoles, achieving miniaturized antenna. Nevertheless, the fractal dipoles extend to two sides of the dipoles in vertical direction, which leads to the result that the spacing factor of Euclidean LPDA is not suitable for design requirements. According to the optimization with the assistance of simulator CST Microwave Studio®, the parameters of PLPTDA are $\tau = 0.85$, $\sigma = 0.15$; the length of the longest dipole arm is $L_1 = l_1/2 = 120\,\text{mm}$, $N = 16$, $l_i/a_i = 125$, $i = 1, 2, 3 \ldots$; the width of dipoles is πa_i; the width of the balanced microstrip feeding line is 3 mm; the relative permittivity and thickness of the FR4 substrate are respectively $\varepsilon_r = 4.4$ and 1.5 mm. The configuration of PLPTDA is shown in Fig. 3(b).

2.2.3. Design of Printed Log-periodic 2nd-iteration Tree-fractal Array ($PLPT^2DA$)

Based on the designed Euclidean LPDA, 2nd-iteration tree-fractal dipoles (noted as T2) are used to take the place of dipoles. Like T1 dipoles, the length of T2 dipoles in co-polarization direction is shorter than that of traditional dipoles, achieving miniaturized antenna. Nevertheless, the fractal dipoles extend to two sides of the dipoles in vertical direction, leading to that the spacing factor of Euclidean LPDA is not suitable for design requirements. According to the optimization with the assistance of simulator CST Microwave Studio®, the parameters of PLPTDA are $\tau = 0.85$, $\sigma = 0.16$; the length of the longest dipole arm is $L_1 = l_1/2 = 120\,\text{mm}$, $N = 16$, $l_i/a_i = 125$, $i = 1, 2, 3 \ldots$; the width of dipoles is πa_i; the width of the balanced microstrip feeding line is 3 mm; the relative permittivity and thickness of the FR4 substrate are respectively $\varepsilon_r = 4.4$ and 1.5 mm. The configuration of PLPTDA is shown in Fig. 3(c).

3. SIMULATED AND EXPERIMENTAL RESULTS AND DISCUSSION

Simulations are conducted by using CST Microwave Studio®. The impedance bandwidth and gain of the zero, first and second iteration LPDAs are shown in Fig. 4. The impedance bandwidth of LPDA (VSWR < 2) is from 0.36 to 2.5 GHz, and gain in this frequency range is from 6.2 to 8.5 dB. The LPDA is an ideal directional ultra-wideband

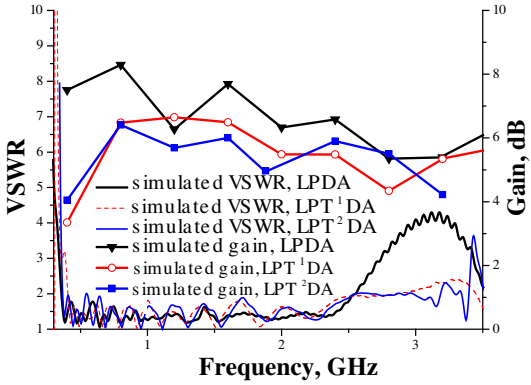

Figure 4. Simulated VSWR and gain of LPDA, LPT^{1}DA and LPT^{2}DA.

antenna. The impedance bandwidth of LPTDA (VSWR < 2) is from 0.4 to 2.85 GHz, and gain in this frequency range is from 4.1 to 7.0 dB. The impedance bandwidth of LPT^{2}DA (VSWR < 2) is from 0.37 to 3.18 GHz, and gain in this frequency range is from 4.0 to 7.0 dB. With the number of iterations increasing, due to mutual coupling brought in by fractal structure, the impedance width increases as well. The ratio bandwidth of the 3 antennas is respectively 6.94 : 1, 7.13 : 1 and 8.59 : 1. The simulated gain shows that the gain of tree-fractal antenna is lower than that of LPDA. On one hand, it is because fractal structure leads to increasing cross-polarization level. On the other hand, it is due to increased mutual coupling. The width of the microstrip feeding line could determine the characteristic impedance, thus it needs to optimize the width carefully. The input impedance of antenna is determined by both feeding line's characteristic impedance and the loading dipoles on feeding line. In order to keep the antenna input impedance to be 50 Ω in broadband range, the width and calculated characteristic impedance of the proposed balanced microstrip feeding line are respectively $w = 3$ mm and 61 Ω.

The start frequencies of the three antennas are the same, so miniaturized effects could be obtained by comparing their sizes. The sizes of these three antennas' substrates are respectively $555 \times 400\,\text{mm}^2$, $570 \times 270\,\text{mm}^2$ and $490 \times 245\,\text{mm}^2$. Compared with Euclidean LPDA, the widths (in co-polarization direction) of LPTDA and LPT^{2}DA are respectively reduced by 32.5% and 38.75%, which achieves the miniaturized effects.

To investigate the validity of the simulations, an LPT^{1}DA and an LPT^{2}DA prototypes were etched on FR4 substrate based on

the optimized parameters with the assistance of simulations. The fabricated antennas are shown in Fig. 3. There is a difference between the simulated and fabricated excitation ports. For simulation purpose, the most appropriate feed is a differential port placed at the narrow (radiating) end of the antenna. In practice, an SMA connector is used for feeding, which is a kind of unbalanced feeding. For miniaturized aim, the antennas are fed without Balun. According to the experimental results, the antennas without Balun feeding have similar performance with the simulated antennas. The experimental environment is microwave anechoic chamber. The characteristics of the fabricated antennas are measured by using an Agilent E8363B Vector Network Analyzer (VNA), and the results are shown in Figs. 5–8. The

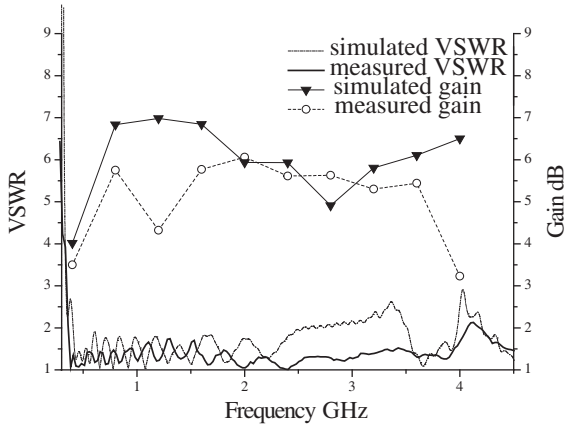

Figure 5. Simulated and measured VSWR and gain of LPT[1]DA.

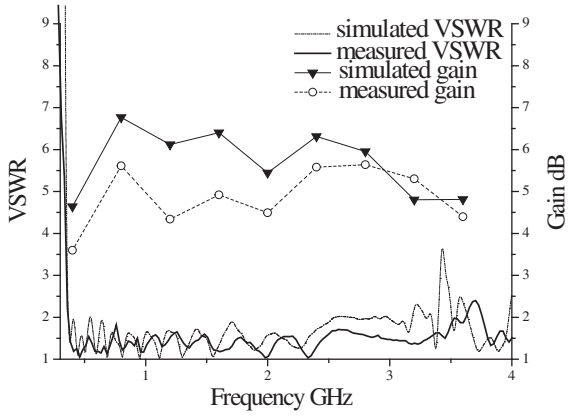

Figure 6. Simulated and measured VSWR and gain of LPT[2]DA.

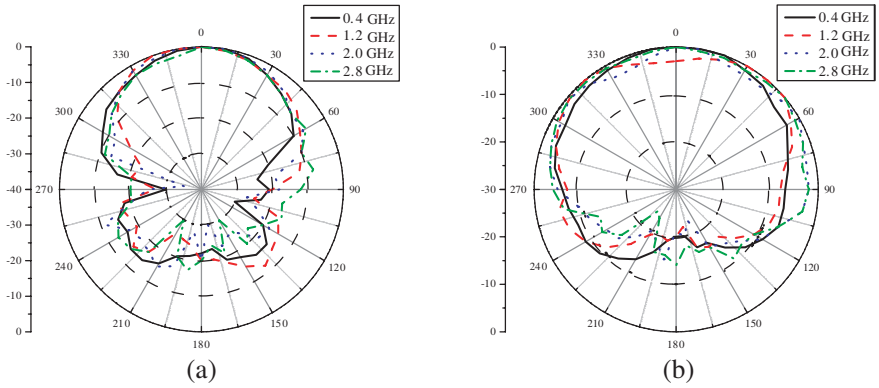

Figure 7. Measured radiation patterns of LPT[1]DA. (a) E-plane. (b) H-plane.

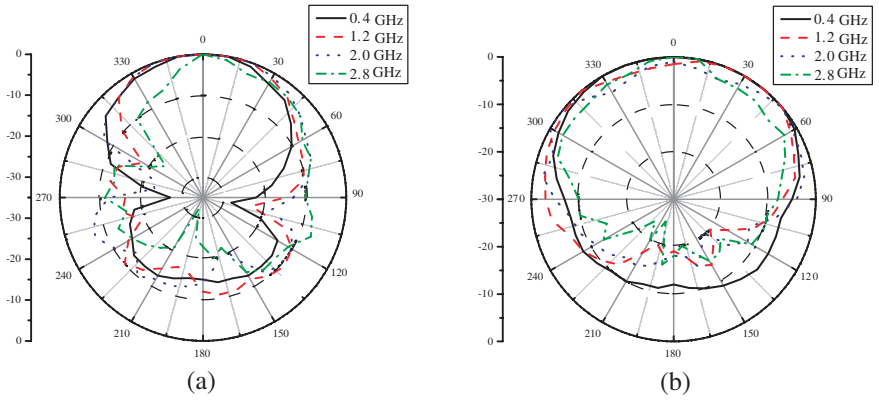

Figure 8. Measured radiation patterns of LPT[2]DA. (a) E-plane. (b) H-plane.

simulation results of the antenna pattern are listed in Fig. 9 and Fig. 10. The measured and simulated results in Figs. 7–9 indicate: (1) The antenna is directional because of the phase difference between dipoles of the periodic log-periodic antenna. (2) The measured and simulated results of the antenna pattern are matched from the variation trend, especially in frequencies of 1.2 GHz and 2.0 GHz. (3) The measured and simulated back lobes differ a lot at frequency 0.4 GHz. This difference is mainly because of the test environment and the influence caused by the test fixture. Additionally, the inhomogeneous distribution of the antenna's medium material (FR4) parameters is also one of the reasons leading to the difference in the measured pattern.

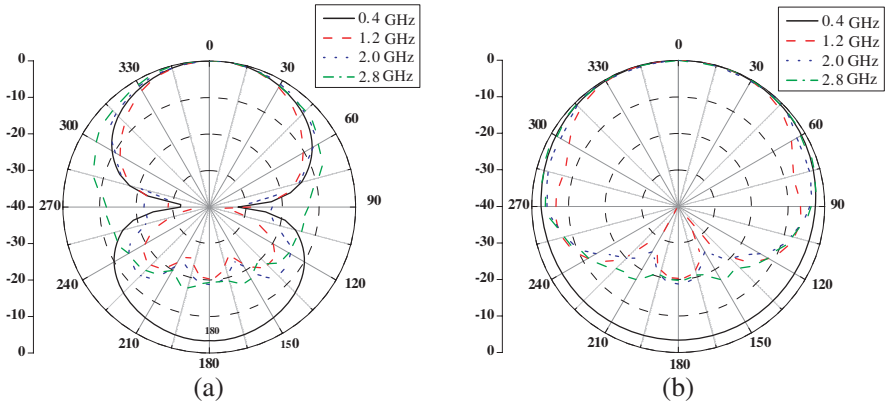

Figure 9. Simulated radiation patterns of LPT[1]DA. (a) *E*-plane. (b) *H*-plane.

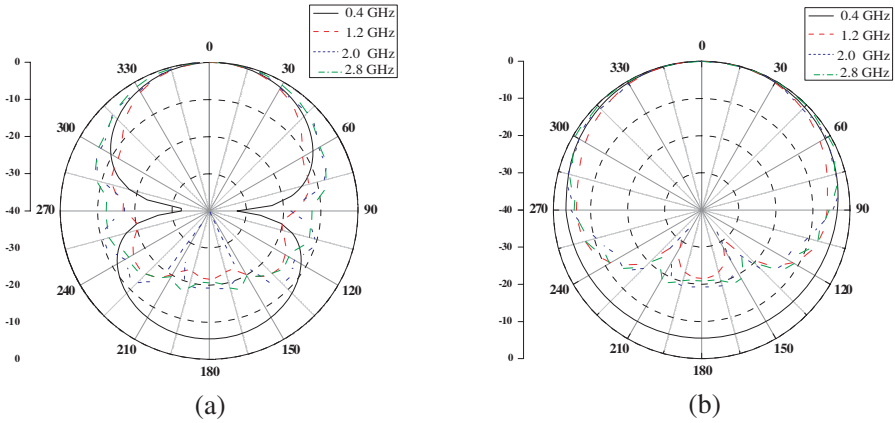

Figure 10. Simulated radiation patterns of LPT[1]DA. (a) *E*-plane. (b) *H*-plane.

The experimental results are as followings: the impedance bandwidths (defined by VSWR < 2) of the PLPT[1]DA and PLPT[2]DA are respectively from 0.36 to 4.1 GHz and from 0.37 to 3.55 GHz, and the total gains are from 3.5 to 6 dB in corresponding bandwidth. Compared with the simulated results, the measured impedance bandwidth is wider, and gain is lower. The differences are mainly caused by the instability of FR4 substrate. For this reason, a loss tangent 0.02 of the substrate was considered in simulations. The new simulated results show that the gain decreases, which proves the

fact that substrate stability affects antenna characteristics (shown in Fig. 11).

Compared with other kinds of antennas shown in [16], the proposed antennas have shorter length in co-polarization direction, due to using 2nd-iteration tree-fractal elements. The LPDAs with similar band width ratio are chosen as comparison objects. Table 1 aims to compare the conductor's length in co-polarization direction and conductor's length in radiation direction, in which electrical length is the main compared data. Compared results show that the proposed antenna has significant miniaturization effects.

There is a lot of free space between dipoles of the ordinary log-periodic antenna. And the phase difference between dipoles is made to generate the directional radiation of the antenna. The space can be fully used because the fractal dipoles have strong space filling performance. Thus the antenna size in the polarization direction (the size in y direction in Fig. 3) can be decreased effectively, while the antenna size in radiation direction (the size in z direction in Fig. 3.) has not changed much.

Additionally, the gains of the LPDA, LPT^{1}DA and LPT^{2}DA at the typical working frequency of 2.0 GHz are 6.7 dB, 5.8 dB and 5.5 dB, which show a descending trend according to the simulation results. The size of the fractal antenna decreases, but the gain also decreases. This is mainly because of adding the coupling among the antenna dipoles.

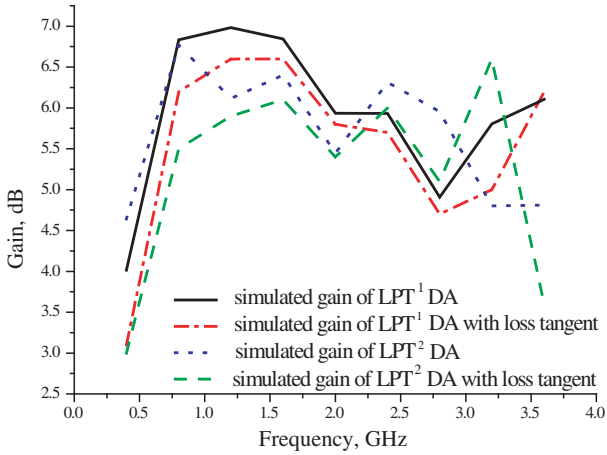

Figure 11. Simulated gain of LPT^{1}DA, LPT^{2}DA and the ones with loss tangent.

Table 1. Parameters of compared antennas.

Miniaturized Antenna	Lowest frequency/GHz	Largest size in co-polarization direction (y direction)/λ_L	Size in radiation direction (z direction)/λ_L	Miniaturization extent
LPMA [16]	2.26	0.828	2.41	165.6%
LPT^{1}DA	0.36	0.324	0.684	64.8%
LPT^{2}DA	0.37	0.302	0.604	60.4%
Ordinary LPDA*	0.36	0.480	0.660	96.0%

*Note: The results of the ordinary LPDA performance in the charm are the simulation values.

4. CONCLUSION

Second-iteration tree-fractal structure is used for the first time in the miniaturization of Euclidean LPDA. The impedance bandwidth (defined by VSWR < 2) of the proposed antenna is from 0.37 to 3.55 GHz with a ratio of above 9.59 : 1. The antenna performance is comparable to a traditional LPDA with similar and directive patterns of constant gain, while the length in co-polarization direction is reduced by about 38%. It is meaningful for antenna miniaturization and invisibility.

The tree-fractal structure has been applied in LPDA, but most of them are limited to 1st-iteration fractal. Through researching on the simulated results of 2nd-iteration tree-fractal dipole, this paper analyzes how tree-fractal iterative times affect the trend of antenna miniaturization and proves that LPT^{2}DA approximates the limitation of antenna miniaturization. As with most antennas, LPTDA has small size at the cost of declining the antenna's performance. By using tree-fractal elements, cross-polarization level and mutual coupling increase, which would lead to gain decline. However, the impedance bandwidth is widened by increasing mutual coupling.

Design procedure of the proposed LPTDA is similar to that of traditional LPDA. It only needs to use tree-fractal dipoles instead of traditional dipoles, then to increase spacing factor appropriately. This design method could also been applied to other fractal LPDA designs. By using stationary mathematic iteration, the corresponding fractal structure could be obtained as dipole elements. Then optimize the antenna parameters by the assistance of simulator or experimental

method. This design procedure makes antenna design relatively simple. The design concept of the proposed antenna can easily be scaled for applications with different bandwidths by changing the number of elements, which is a miniaturized antenna modeling with a bright application prospect.

ACKNOWLEDGMENT

The authors would like to express their sincere gratitude to CST Ltd., Germany, for providing the CST Training Center (Northeast China Region) at our university with a free package of CST MWS software.

The authors would like to express their sincere gratitude to "the Fundamental Research Funds for the Central Universities" (Grant No. HIT.NSRIF. 2010096) and the funds supported by "Heilongjiang post-doctorial financial assistance (LBH-Z09187)".

REFERENCES

1. Liang, J., C. C. Chiau, X. Chen, and C. G. Parini, "Printed circular disc monopole antenna for ultra-wideband applications," *Electronics Letters*, Vol. 40, No. 20, 1246–1247, 2004.
2. Nikolaou, S., N. D. Kingsley, G. E. Ponchak, J. Papapolymerou, and M. M. Tentzeris, "UWB elliptical monopoles with a reconfigurable band notch using MEMS switches actuated without bias lines," *IEEE Transactions on Antennas and Propagation*, Vol. 57, No. 8, 2242–2251, 2009.
3. Gayathri, R., T. U. Jisney, D. D. Krishna, M. Gopikrishna, and C. K. Aanandan, "Band-notched inverted-cone monopole antenna for compact UWB systems," *Electronics Letters*, Vol. 44, No. 20, 1170–1171, 2008.
4. Ye, L.-H. and Q.-X. Chu, "Improved band-notched UWB slot antenna," *Electronics Letters*, Vol. 45, No. 25, 1283–1285, 2009.
5. Lizzi, L., F. Viani, R. Azaro, and A. Massa, "A PSO-driven spline-based shaping approach for ultra wideband (UWB) antenna synthesis," *IEEE Transactions on Antennas and Propagation*, Vol. 56, No. 8, 2613–2621, 2008.
6. Gibbins, D., M. Klemm, I. J. Craddock, J. A. Leendertz, A. Preece, and R. Benjamin, "A comparison of a wide-slot and a stacked patch antenna for the purpose of breast cancer detection," *IEEE Transactions on Antennas and Propagation*, Vol. 58, No. 3, 665–674, 2010.

7. Dastranj, A., A. Imani, and M. Naser-Moghaddasi, "Printed wide-slot antenna for wideband applications," *IEEE Transactions on Antennas and Propagation*, Vol. 56, No. 10, 3097–3102, 2008.
8. Deng, C. and Y. J. Xie, "Design of resistive loading Vivaldi antenna," *IEEE Antennas and Wireless Propagation Letters*, Vol. 8, 240–243, 2009.
9. Chung, K. H., S. H. Pyun, and J. H. Choi, "Design of an ultrawideband TEM horn antenna with a microstrip-type balun," *IEEE Transactions on Antennas and Propagation*, Vol. 53, No. 10, 3410–3413, 2005.
10. Venkatesan, V. and K. T. Selvan, "Rigorous gain measurements on wide-band ridge horn," *IEEE Transactions on Electromagnetic Compatibility*, Vol. 48, No. 3, 592–594, 2006.
11. Zhou, Z. W., S. W. Yang, and Z. P. Nie, "A novel broadband printed dipole antenna with low cross-polarization," *IEEE Transactions on Antennas and Propagation*, Vol. 55, No. 11, 3091–3093, 2007.
12. Campbell, C. K., I. Traboulay, M. S. Suthers, and H. Kneve, "Design of a strip line log periodic dipole antenna," *IEEE Transactions on Antennas and Propagation*, Vol. 25, No. 5, 718–721, September 1977.
13. Sundaram, A., M. Maddela, and R. Ramadoss, "Koch-fractal folded-slot antenna characteristics," *IEEE Antennas and Wireless Propagation Letters*, Vol. 6, 219–222, 2007.
14. Petko, J. S. and D. H. Werner, "Miniature reconfigurable three-dimensional fractal tree antennas," *IEEE Transactions on Antennas and Propagation*, Vol. 52, No. 8, 1945–1956, 2004.
15. Murad, N. A., M. Esa, M. Fairus, M. Yusoff, S. Hajar, and A. Ali, "Hilbert curve fractal antenna for rfid application," *International RF and Microwave Conference Proceedings*, 182–186, Putrajaya, Malaysia, September 12–14, 2006.
16. Wu, Q., R. H. Jin, and J. P. Geng, "A single-layer ultrawideband microstrip antenna," *IEEE Transactions on Antennas and Propagation*, Vol. 58, No. 1, 211–214, 2010.